Russian Chemical Reviews **65** (3) 181 – 195 (1996)
© 1996 Russian Academy of Sciences and Turpion Ltd

UDC 541.138

Electrochemistry of hydride-forming intermetallic compounds and alloys

O A Petrii, S Ya Vasina, I I Korobov

Contents

I.	Introduction	181
II.	Brief history of the discovery and use of hydride-forming intermetallic compounds	181
III.	The main types of metal hydride electrodes	182
IV.	The technology of the manufacture and activation of metal hydride electrodes	187
V.	Hydrogen evolution reaction on metal hydride electrodes	188
VI.	Charge – discharge processes on metal hydride electrodes	189
VII.	Corrosion of metal hydride electrodes	191
VIII.	Conclusion	193

Abstract. The present review covers studies published over the past 15 years on the electrochemistry of hydride-forming intermetallic compounds (IMC) and alloys. Data on the discharge capacity and stability of electrode materials based on IMC and AB, AB_2, AB_3 and AB_5 type alloys and their substituted derivatives during potential cycling are classified and generalised. The problems concerning the optimisation of the elemental composition of IMC and alloys, their production and activation as well as the reasons for the degradation of electrodes based on these materials are discussed. The mathematical models suggested for describing the processes of discharge and degradation of metal hydride electrodes are analysed. The bibliography includes 149 references.

I. Introduction

It was found in the 1960s that a series of intermetallic compounds (IMC) possess the unique capability to absorb reversibly an anomalously large amount of hydrogen (up to 1.5% – 2%)† at moderate pressures and temperatures.[1] This led to the appearance of several new fields of scientific investigations directly related to the solution of problems of hydrogen energetics and technology. The results of these studies show the possibility of developing methods, new in principle, for the preparation, storage, purification, compression and application of hydrogen in different technological processes and energy-transforming systems.[1,2]

The present review deals with electrode materials based on hydride-forming IMC and alloys with a high sorption capacity for hydrogen. These materials are primarily intended for use in nickel – metal hydride batteries. Palladium was the first hydride-forming element to attract the particular attention of electrochemists after studies by Nilen[3] and Frumkin.[4,5] Palladium has since been extensively used as a classical model in hydride electrochemistry, since processes of hydrogen sorption – desorption, reversible at ambient temperature but not complicated by corrosion phenomena, can be implemented only with this material. The recent commercial use of hydrides was preceded by extensive studies of a wide range of new materials, which makes it urgent to analyse and generalise the data obtained to date.

In this review we consider the main aspects of the electrochemistry of hydride-forming materials that have attracted most research attention in recent years and that we believe to be of interest to a wide circle of chemists.

† The content of hydrogen in these materials (v/v) is 1.5 to 2 times higher than in liquid hydrogen.

O A Petrii, S Ya Vasina M V Lomonosov Moscow State University, Chemistry Department, 119899 Moscow, Russian Federation.
Fax (7-095) 939 27 42. Tel. (7-095) 939 13 21, (7-095) 939 53 75.
I I Korobov Institute of New Chemical Problems, Russian Academy of Sciences, 142432 Chernogolovka, Russian Federation.
Fax (7-095) 524 50 24.

Received 13 June 1995
Uspekhi Khimii **65** (3) 195 – 210 (1996); translated by S S Veselyi

II. Brief history of the discovery and use of hydride-forming intermetallic compounds

The first studies on the use of hydride-forming IMC as reversible electrodes carried out by Justi et al.[6] for individual compounds of the $Ti_{1-x}Ni_x$ system, and by Gutjahr et al.[7] for a mixture of intermetallic compounds Ti_2Ni – TiNi, have demonstrated, in principle, the possibility of the cathodic storage of hydrogen using these IMC.

In 1973, the results of a study on the electrochemical behaviour of $LaNi_5$ were reported.[8] This compound was found to have a discharge capacity of 200 mA h g^{-1}, which, however, was much lower than the value expected from the pressure – composition isotherm for the $LaNi_5 - H_2$ system (360 mA h g^{-1}). In 1975, the first battery with $LaNi_5$ as a metal hydride cathode was patented.[9]

During the following years, the main attention of researchers was devoted to increasing the electrochemical capacity of metal hydride (MH) electrodes and to decreasing the loss of capacity in storage (self-discharge). With this purpose, IMC of the $LaNi_5$ type with partial replacement of lanthanum and nickel by other metals, whose electrochemical charging results in hydride phases with lower equilibrium dissociation pressures, have been studied.[10-12]

It was found that the main difficulty in the use of such IMC as TiNi, Ti_2Ni, $LaNi_5$, $MmNi_5$ (Mm is 'mischmetall', i.e., a technical mixture of rare-earth metals) and their substituted derivatives as MH electrodes in batteries was the low stability of the IMC under electrochemical charge – discharge cycling conditions due to degradation processes.

Since the early '80s, studies in the field of MH electrodes have been directed at increasing the stability of AB_5 type IMC under cycling conditions (requiring the development of multicomponent alloys maintaining the initial hexagonal structure of the $CaCu_5$ type),[13] on the one hand, and at the search for electrochemically new species, i.e., IMC of the AB_3 type and the substituted derivatives,[14,15] multicomponent Laves phases of AB_2 stoichiometry,[16,17] hyperstoichiometric compounds of AB_{5+x} [18,19] and AB_{2+x} types,[17,20-22] IMC in amorphous, nanocrystalline forms and IMC films.[23-26]

III. The main types of metal hydride electrodes

The adsorption and desorption of gaseous hydrogen on IMC are described by $P-T-c$ diagrams, while those on MH electrodes are described by charge-discharge curves, i.e., plots of electrode potential *versus* the quantity of electricity passed (Q).

The charging of MH electrodes in alkaline electrolytes occurs because the electrochemical reduction of water gives hydrogen, which is then absorbed by the IMC. During discharge, hydrogen diffuses from the bulk of the IMC to the electrode surface and is oxidised. The electrochemical adsorption–desorption of hydrogen by AB_x compounds can therefore be represented by the following general equation:

$$AB_x + yH_2O + y\bar{e} \rightleftarrows AB_xH_y + yOH^-.$$

A charge of one electron corresponds to each absorbed hydrogen atom, and the charge–discharge capacity (C) per unit mass (m) is determined by the equation:

$$C = \frac{Q}{m}.$$

The charge–discharge curves used for the determination of the full hydrogen capacity of electrodes (C^0_{eq}) should be recorded under equilibrium conditions, i.e., at very low charge or discharge currents. In practice, after passing a certain amount of electricity, it is necessary to disconnect the circuit and record the currentless (equilibrium) potential, and then plot graphically the dependence of the amount of electricity passed on the currentless potential. This procedure makes it possible to avoid errors related to the retardation of hydrogen diffusion into the bulk of the electrode and of other steps. In most studies, the full capacity values (C^0) were obtained under nonequilibrium conditions: first, the capacity was determined at high discharge currents (C_h), then the current was diminished (usually, tenfold), and the capacity was determined at low current (C_l). The full capacity is calculated as $C_h + C_l$.

The equilibrium potential of an MH electrode is related to the equilibrium pressure in the adsorption and desorption of hydrogen (p_{H_2}) by the Nernst equation

$$E_r = -\frac{RT}{2F}\ln p_{H_2}, \quad (1)$$

where E_r is the potential of the MH electrode relative to the reversible hydrogen electrode in the same solution. Thus, the equilibrium hydrogen pressure over the hydride phase that characterises the stability of the latter can be calculated from the potential corresponding to a plateau on equilibrium charge–discharge curves. The main requirements that should be met by MH electrodes used in current sources are high discharge capacity and cyclic stability during electrochemical charge and discharge, $S(N)$

$$S(N) = \frac{C(N)}{C^0}100\,(\%), \quad (2)$$

where $C(N)$ in the discharge capacity at the Nth cycle.

Table 1 presents the currently available literature data on the studies of IMC and various alloys, i.e., AB, AB_2, AB_3, AB_5 and their substituted derivatives, as MH electrodes.

1. $LaNi_5$ and its substituted derivatives

$LaNi_5$ is an intermetallic compound which has been the most frequently studied electrochemically as an MH electrode. It is characterised by a high discharge capacity (in closed electrochemical cells), electrocatalytic activity and corrosion resistance in alkaline electrolytes. However, despite all of these advantages, $LaNi_5$ has a significant drawback, *viz.* low cyclic charge–discharge stability due to degradation processes, the mechanism of which will be considered below.

The partial replacement of Ni in $LaNi_5$ by Mn, Cu, Cr, Al or Co, which have higher atomic radii than that of nickel, enables the synthesis of IMC with lower equilibrium dissociation pressures of the hydride phases (< 0.098 MPa) with retention of the hexagonal type of the lattice. For example, the replacement of one nickel atom by one aluminium atom decreases p_{H_2} by almost three orders of magnitude.[27] Hence, MH electrodes based on such IMC have lower self-discharge due to the desorption of hydrogen as a gas under atmospheric pressure.

A comparison of $S(N)$ values and relative increases in the unit cell volume upon hydrogenation ($\Delta V/V$) showed[13,27] that alloys, the hydrogenation of which results in insignificant volume increase, have the highest stability. Unfortunately, such alloys normally have low discharge capacity, while both of these parameters should be taken into account in the selection of MH electrode composition.

The considerable increase in the cyclic stability of $LaNi_5$ when alloyed with cobalt was first noted by Willems.[13] The effect of the replacement of nickel by cobalt is enhanced when a small amount of silicon or aluminium is added[13,34] due to the formation of a protective oxide layer on the surface. The presence of this layer, which hinders hydrogen diffusion into the bulk of the metal, increases the overvoltage of the electrochemical charge-discharge of the electrode. The addition of titanium increases the cyclic stability, but simultaneously decreases markedly the electrochemical capacity, unlike neodymium, which increases this parameter. According to the data of Sakai and co-workers[34], an alloy in which there is partial replacement of lanthanum by neodymium and of cobalt by aluminium, viz. $La_{0.8}Nd_{0.2}Ni_{2.5}Co_{2.4}Al_{0.1}$, is the most suitable MH electrode [$C^0 = 241$ mA h g^{-1}, $S(300) = 85\%$].

The partial replacement of lanthanum by zirconium and of nickel by aluminium in $LaNi_5$ considerably prolongs the operation time of MH electrodes. The optimum compositions correspond to the formula $La_{1-x}Zr_xNi_{4.5}Al_{0.5}$, where $x = 0.1-0.2$.[37]

2. $MmNi_5$ and its substituted derivatives

The price of industrially manufactured $LaNi_5$ on the world market is ~$30 US per kg.[39] The cost of MH electrodes can be reduced considerably if the lanthanum in the IMC is completely or partly replaced by 'mischmetall'. However, this replacement increases the dissociation pressure of the hydride phases. For example, this value is ~1.5 MPa at 298 K for $MmNi_5$.[40]

To decrease the equilibrium pressure over the hydride phase in $MmNi_5$, as in the case of $LaNi_5$, it is necessary to partly replace nickel by such metals as aluminium or manganese.[28,41] It was found that $MmNi_5$ should be alloyed not only with aluminium or manganese, but also with cobalt in order to enhance the cyclic stability of MH electrodes.[41,43] It is remarkable that a profound effect is observed upon replacement of as little as one nickel atom by a cobalt atom, whereas the optimum replacement number for $LaNi_5$ is from 2 to 2.5 nickel atoms. This may be connected with the presence of Ce in the Mm.

The general criteria for selection of the IMC composition of the $MmNi_5$ type are the same as in the case of $LaNi_5$, and the optimum compositions differ only in the quantity of components added (see Table 1).

Table 1. The main types of MH electrodes based on hydride-forming intermetallic compounds (IMC) and alloys.

IMC	C^0 / mA h g^{-1}	$S(N)$ (%)	Ref.
$LaNi_5$ and its substituted derivatives			
$LaNi_5$	350 – 372	12 – 15 (400)	12, 13, 19, 28, 29
	250 – 275	26 (150)	27, 91
$LaNi_{4.5}Mn_{0.5}$	318	17 (150)	27
	315	40 – 60 (100)	30
$LaNi_4Mn$	220	31 (150)	27
$LaNi_{4.5}Cu_{0.5}$	250	36 (150)	27
$LaNi_4Cu$	260 – 270	27 (150)	12, 27
	342 – 373	16 (400)	19, 28, 29
$LaNi_{4.5}Cr_{0.5}$	286	41 (150)	27
$LaNi_4Cr$	174; 280	67 (150)	12, 27
$LaNi_{5-x}Al_x$	355 – 185	16 (400) ($x = 0.1$)	13, 27, 28, 31
$x = 0.1 - 1.0$		56 (150) ($x = 0.5$)	32
		100 (150) ($x = 1$)	27
$LaNi_{5-x}Co_x$	372 – 273	25 – 64 (400)	13
$x = 1.0 - 3.3$			
$LaNi_{2.5}Co_{2.5}$	230	90 (150)	27
	244 – 264	57 (300)	33, 34
$LaNi_{4.5}Fe_{0.5}$	320	40 (200)	35
$LaNi_{4.9-x}Co_xAl_{0.1}$	365 – 289	30 – 94 (400)	13
$x = 2.5 - 3.0$			
$LaNi_{2.5}Co_{2.4}Al_{0.1}$	231	83 (300)	34
$LaNi_{4.7}Si_{0.3}$	270		36
$LaNi_{4.9-x}Co_xSi_{0.1}$	350 – 280	33 – 96 (400)	13
$x = 1.0 - 3.0$			
$LaNi_{2.5}Co_{2.4}Si_{0.1}$	230	76 (300)	34
$LaNi_{2.5}Co_{2.4}Mn_{0.1}$	244		33
$LaNi_{4.4}Al_{0.3}Si_{0.3}$	270		36
$La_{0.8}Nd_{0.2}Ni_2Co_3$	302	48 (400)	13
$La_{0.7}Nd_{0.3}Ni_{2.5}Co_{2.4}Al_{0.1}$	293	87 (400)	13
$La_{0.8}Nd_{0.2}Ni_{2.5}Co_{2.4}Al_{0.1}$	241	85 (300)	34
$La_{0.8}Nd_{0.2}Ni_{2.5}Co_{2.4}Si_{0.1}$	293	88 (400)	13
	280	30 (1000)	29
$La_{0.7}Nd_{0.2}Ti_{0.1}Ni_{2.5}Co_{2.5}$	178	90 (300)	34
$La_{0.7}Nd_{0.2}Ti_{0.1}Ni_{2.5}Co_{2.4}Al_{0.1}$	175	94 (300)	34
$La_{0.7}Nd_{0.2}Ti_{0.1}Ni_{2.5}Co_2Al_{0.5}$	254	90 (400)	13
$La_{0.7}Nb_{0.3}Ni_{2.5}Co_{2.4}Cr_{0.1}$	186		33
$La_{0.9}Zr_{0.1}Ni_5$	137	50 (440)	37
$La_{0.8}Zr_{0.2}Ni_5$	140	50 (540)	37
$La_{0.9}Zr_{0.1}Ni_{4.5}Al_{0.5}$	300 – 350	75 (300)	38
	280	50 (580)	37
$La_{0.85}Zr_{0.15}Ni_{4.5}Al_{0.5}$	271	50 (690)	37
$La_{0.8}Zr_{0.2}Ni_{4.5}Al_{0.5}$	254	50 (810)	37
$La_{0.8}Ce_{0.2}Ni_2Co_3$	267	84 (265)	33
$MmNi_5$ and its substituted derivatives			
$MmNi_5$	170		40
$MmNi_4Mn$	350	30 (700)	41
$MmNi_4Al$	214; 280		28, 41
$MmNi_4Co_{0.7}Al_{0.3}$	300		41
	200 – 300		42
$MmNi_{3.5}Co_{0.7}Al_{0.8}$	240; 200;	95 (1000)	43, 44
	183; 250	92 (2000)	33, 45
$Mm_{1.1}Ni_{3.25}CoAl_{0.75}$	220	65 (600)	41
$MmNi_{3.25}(CoMn)_{1.75}$	220	65 (700)	41
$MmNi_{3.45}(CoMnTi)_{1.55}$	300	87 (540)	41
		77 (1000)	
$MmNi_{3.55}Co_{0.75}Al_{0.3}Mn_{0.4}$	240		46
$Mm(Ni_{3.6}Co_{0.7}Al_{0.3}Mn_{0.4})_{0.92}$	210		28
$MmNi_{4.49}Co_{0.1}Al_{0.205}Mn_{0.205}$	330		47
$MmNi_{4.2}Mo_{0.6}Al_{0.2}$		80 (150)	48
$MmNi_{3.7}Al_{0.5}Fe_{0.7}Cu_{0.1}$	220	Reserve of	49
		60 cycles ($N = 60$)	
$MmNi_xCu_aMn_bAl_c$	250 – 300	Reserve of	50
$3.5 < x < 4.3$; $0.2 < a < 1.2$;		200 cycles ($N > 200$)	
$0.15 < b < 0.85$; $0.05 < c < 0.5$			
$Mm_{0.5}La_{0.5}Ni_2Co_3$	156		33

Table 1 (continued).

IMC	C^0 / mA h g^{-1}	$S(N)$ (%)	Ref.
$Mm_{0.8}Ti_{0.1}Zr_{0.1}Ni_{4.8}Si_{0.2}$	298	Reserve of 300 cycles (N = 300)	51
$Mm_{0.8}Zr_{0.2}Ni_4Al$	240	40 (700)	41
$Mm_{0.9}Ti_{0.1}Ni_{3.9}Co_{0.4}Al_{0.3}Mn_{0.4}$	259	65 (200)	52
$Ln_{1-x}M_xNi_{5-y}M'_y$ Ln = La or Mm; M = Ti, Y, Zr, Nb, Mo, Hf, Ta, Th, Ba, Ca; M′ = Si, V, Fe, Co, Zn, Mg, Ca, Ba, Cu, Mn, Al, Mo, Cr, Sn, Sb	250 – 300	Reserve of 160 – 200 cycles (N = 160 – 200)	51 – 55
$MmNi_{3.7}Al_{0.8}Si_{0.5}$	100		36
$Mm_{0.5}La_{0.5}Mn_{0.2}Ni_{4.2}Al_{0.3}Si_{0.3}$	270		36
$ML_{0.6}La_{0.4}(NiAlCu)_{4.2}Co_{0.8}$ ML — Mm, enriched with La	270	97.5 (100)	56
$ML_{0.5}Mm_{0.5}Ni_4Mn_{0.2}Al_{0.5}Si_{0.3}$	200		36
Hyperstoichiometric IMC of $AB_{(5+x)}$ type			
$LaNi_{5.4}$	360	25 (400)	19
$LaNi_{4.2}Cu$	360	62 (400)	19
$LaNi_{4.4}Cu$	285	90 (400)	19
$LaNi_5Cu$	198	98 (400)	19
$LaNi_{4.9}Cu_{0.5}$	306	63 (400)	19
$LaNi_{4.6}Cu_{0.5}$	282	81 (400)	19
$LaNi_{3.9}Cu_{1.5}$	281	83 (400)	19
$LaNi_{3.4}Cu_2$	245	89 (400)	19
$LaNi_{2.9}Cu_{2.5}$	230	87 (400)	19
$LaNi_{2.4}Cu_3$	230	73 (400)	19
$La_{0.8}Nd_{0.2}Ni_3Co_{2.4}Si_{0.1}$	276	84 (400)	18
$La_{0.8}Nd_{0.2}Ni_{2.9}Co_{2.4}Mo_{0.1}Si_{0.1}$	285	73 (400)	18
Intermetallic compounds of AB_3 type and their substituted derivatives			
$CeNi_{3-x}Co_x$; x = 0, 1, 2	160		14
$YNi_{2.5}M_{0.5}$ M = Ni, Al, Fe, Cr, Cu, Co, Mn	150 – 200		15
(Ti, Zr) – Ni alloys			
TiNi	250		6
Ti_2Ni	250		6
$TiNi + Ti_2Ni$	320		7
$Ti_{1-x}Zr_xNi_y$ x = 0.2 – 0.8; y = 0.5 – 1	450 – 250		60
$Ti_{0.6}Zr_{0.4}Ni_{0.75}$	180 – 200	50 (120)	61
$Ti_{0.5}Zr_{0.5}Ni$	180 – 200	50 (240)	61
$Ti_{0.5}Zr_{0.5}Ni_{0.95}Cu_{0.05}$	180 – 200	50 (360)	61
$Ti_{0.5}Zr_{0.5}Ni_{0.9}Cu_{0.1}$	180 – 200	50 (630)	61
$Ti_{0.2}Zr_{0.8}Ni_{1.25}$	180 – 200	50 (1200)	61
$ZrNi_{1.45}$	180 – 200	50 (2230)	61
$ZrNi_{1.43}$	285		62
$ZrNi_2$	182		63
Laves phases with AB_2 stoichiometry and with hyperstoichiometric composition			
$TiV_3Ni_{0.56}$	420		64
$ZrNi_{2-x}V_x$ x = 0.1 – 0.8	113 – 345		63
$ZrNi_{1.5}V_{0.5}$	345	60 (300)	63
	240	75 (180)	59
	300 – 600		65
$Zr(Ni_{0.67}V_{0.33})_2$	218 – 297	57 (100)	17
$Zr_{1.6-1.7}Ti_{2-1}V_{2.6-5.4}Ni_{4.7-2.3}$	350 – 265		16
$Zr_{0.9}Ti_{0.1}(V_{0.33}Ni_{0.67})_2$	273	57 (100)	17
$Zr(V_{0.33}Ni_{0.67})_{2.4}$	304 – 311	57 (100)	17
	200		21
$Zr_{0.9}Ti_{0.1}(V_{0.33}Ni_{0.67})_{2.4}$	262 – 264	57 (100)	17
$Zr(V_{0.33}Ni_{0.59}Co_{0.08})_{2.4}$	326	57 (100)	17
$Zr(V_{0.33}Ni_{0.5}Co_{0.17})_{2.4}$	328	57 (100)	17
$Zr(V_{0.33}Ni_{0.59}Fe_{0.08})_{2.4}$	332	57 (100)	17
$Zr(V_{0.33}Ni_{0.59}Mn_{0.08})_{2.4}$	363	57 (100)	17
$Zr(V_{0.33}Ni_{0.5}Mn_{0.17})_{2.4}$	366	57 (100)	17
$Zr_{0.9}Ti_{0.1}(V_{0.33}Ni_{0.59}Co_{0.08})_{2.4}$	314 – 316	57 (100)	17
$ZrNi_{1.2}Mn_{0.8-x}Cr_x$ x = 0.2 – 0.8	200 – 300		57, 58

Table 1 (continued).

IMC	C^0 / mA h g^{-1}	$S(N)$ (%)	Ref.
$Zr_yNi_{1.2}Mn_{0.4}Cr_{0.4}$ $y = 0.8 - 1.2$	200		57
$ZrNi_{1.2}Mn_{0.5}Cr_{0.2}V_{0.1}$	340		57
$ZrNi_{1.2}Mn_{0.3}Cr_{0.2}V_{0.3}$	360		57
$ZrNi_{1.2}Mn_{0.4}Cr_{0.4}$	250		57
$ZrNi_{1.2}Cr_{0.8}$	330		57
$Zr_{0.5}Ti_{0.5}NiV$	350	50 (10)	59
$Zr_{0.5}Ti_{0.5}Ni_{1.25}V_{0.75}$	270	50 (120)	59
$Zr_{0.5}Ti_{0.5}Ni_{1.3}V_{0.7}$	280	28 (70)	59
$Zr_{0.5}Ti_{0.5}Ni_{1.5}V_{0.5}$	250	72 (170)	59
$Zr_{0.6}Ti_{0.4}Ni_{1.5}V_{0.5}$	260	58 (140)	59
$Zr_{0.5}Ti_{0.5}Ni_{1.1}V_{0.75}Fe_{0.15}$	250	88 (70)	59
$Zr_{0.5}Ti_{0.5}Ni_{1.1}V_{0.75}Cr_{0.15}$	210	100 (70)	59
$Zr_{0.5}Ti_{0.3}Ni_{1.1}V_{0.75}Cr_{0.3}$	330		66
$TiNi_{0.6-0}V_{0.64}Mn_{0.61-1.21}Fe_{0.15}$	137 – 160		67
$Ti_{0.8}Zr_{0.2}Ni_{0.6}V_{0.64}Mn_{0.61}Fe_{0.15}$	154		67
$ZrCr_{0.8}M_{0.2}NiMm_{0.05}$ M = V, Mn, Fe, Co	300 – 370		22
$Zr(V-Mn-Ni-Mo)_{2.4}$	300		20
$Zr_{0.5}Ti_{0.5}Ni_{1.3}V_{0.7}M_{0.2}$ M = Fe, Cr, Mn	200 – 300		24
$Zr_{0.5}Ti_{0.5}V_{0.75}Ni_{1.5}$	294	85 (1000)	68
$Zr_{0.9}Ti_{0.1}(Ni_{0.51}V_{0.33}Co_{0.08}Mn_{0.08})_2$	240		21
$CeNi_2$	81	91 (500)	69
$PrNi_2$	71	84 (500)	69
$LaNi_2$	70	100 (500)	69
$MmNi_2$	61	79 (500)	69

3. Nonstoichiometric intermetallic compounds AB_{5+x}

In the early 1990s, the first reports appeared[18,70–73] on the electrochemical behaviour of hydrogen-absorbing nonstoichiometric alloys. It was assumed[72,73] that a portion of the La atoms in the crystal lattice of $LaNi_5$ can be replaced by B atoms (one La atom is replaced by two B atoms) to form a new class of nonstoichiometric compounds AB_x, where $x > 5$.

The first compounds studied were two-phase.[20,74] In addition to the AB_5 phase, they contained a second, electrochemically highly reactive phase homogeneously distributed at the grain boundaries of the main alloy. This second phase contained transition metals; it was difficult to predict its composition, although it was undoubtedly determined by the thermodynamic stability of the corresponding compounds.

A detailed study[18] of $AB_{5.5}$ type IMC, such as $La_{0.8}Nd_{0.2}Ni_3Co_{2.4}Si_{0.1}$ and $La_{0.8}Nd_{0.2}Ni_{2.9}Mo_{0.1}Co_{2.4}Si_{0.1}$, using scanning electron microscopy, optical microscopy, and electron microanalysis showed that cooling of homogeneous alloys resulted in the formation of grains of an AB_5 type of hydride-forming alloy, $NiCo_3$ (in the former case) or $MoCo_3$ (in the latter case) being distributed at the grain boundaries. It is likely that it is the presence of these phases that results in a two- to threefold increase in the exchange current density of the hydrogen evolution reaction, since, according to the Brewer–Engel[75] valence bond theory, the simultaneous presence of Ni and Co or Mo and Co can cause a synergistic effect.

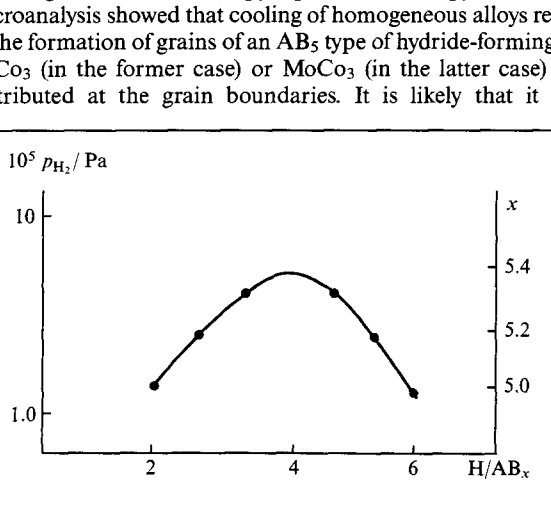


Figure 1. Phase diagram for Cu-containing $AB_x - H_2$ ternary systems.[19]

Such properties as the capacity and the cycling stability of two-phase and of the corresponding single-phase systems are similar, since they are determined by the main alloy. However, the discharge properties of two-phase systems are significantly better.

Later, single-phase nonstoichiometric alloys were obtained by the homogenising annealing of $La(NiCu)_x$ alloys, where $5 \leqslant x \leqslant 6$, and their electrochemical characteristics were studied.[19] It was found that an increase in x increases the annealing temperature required for obtaining single-phase samples, decreases the discharge capacity, and lengthens the activation process. However, the cyclic stability of electrodes is improved considerably: the residual discharge capacities of $LaNi_4Cu$ and $LaNi_5Cu$ after 400 charge-discharge cycles are 16% and 98%, respectively.

Based on measurements of the adsorption isotherms of gaseous hydrogen, a phase diagram of Cu-containing $AB_x - H_2$ ternary systems was plotted (Fig. 1).[19] The region of coexistence of α- and β-hydride phases rapidly narrows as x increases and completely disappears at a certain 'critical' composition that approximately corresponds to the formula $LaNi_{4.4}Cu$. The isotherm of hydrogen sorption by this compound contains almost no horizontal plateau corresponding to the $\alpha \rightleftarrows \beta$ transition.

4. Intermetallic compounds of AB_3 type and their substituted derivatives

The electrochemical behaviour of the IMC of the composition AB_3 has has so far been studied only for the $CeNi_{3-x}Co_x$ and $YNi_{3-x}M_x$ systems, where M = Al, Fe, Co, Cu, Mn and Cr.[14,15,76–78] Increase in the cobalt content of $CeNi_{3-x}Co_x$ increases the thermodynamic stability of the corresponding hydride phases and decreases the equilibrium dissociation pressure from 0.5×10^3 Pa for $CeNi_3$ to 0.2×10^3 Pa for

$CeNiCo_2$ at 293 K.[14] The electrochemical charge–discharge processes of the IMC of this system follow the equation

$$CeNi_{3-x}Co_xH_3 \rightleftarrows CeNi_{3-x}Co_xH + H_2.$$

Because a stable monohydride of the IMC is formed, the reversible electrochemical capacity of these MH electrodes is lower than that of $LaNi_5$ and $MmNi_5$ electrodes.

The partial replacement of Ni in YNi_3 by Al, Co, Fe, Mn, Cr, or Cu has almost no effect on the reversible electrochemical capacity but increases (except for Cr) the equilibrium dissociation pressure of the corresponding hydride phases.[15]

5. Ti–Ni alloys and their substituted derivatives

Ti–Ni alloys were the first materials studied as MH electrodes.[6,7] The electrochemical charging capacity of the Ti_2Ni alloy is 425 mA h g^{-1}, which corresponds to the formation of the hydride $Ti_2NiH_{2.5}$. On the other hand, the discharge capacity is considerably lower (250 mA h g^{-1}), i.e. part of the hydrogen (~1 mol) is not available electrochemically. Unlike Ti_2Ni, the intermetallic compound TiNi is a totally reversible electrode with a discharge capacity of 250 mA h g^{-1}.

When equimolar amounts of TiNi and Ti_2Ni are present simultaneously, the reversible electrochemical capacity of the system increases to 320 mA h g^{-1}, which corresponds to the oxidation of ~85% of the hydrogen; the final composition of the system is $Ti_2NiH_{0.5}$ + TiNi. It was assumed[7] that the complete discharge of TiNiH into TiNi with simultaneous partial discharge of the $Ti_2NiH_{2.5}$ phase occurs in the first step, and then redistribution of hydrogen between the Ti_2NiH_x phase and TiNi takes place along with its further electrochemical oxidation, i.e. the TiNi phase has a specific 'catalytic' effect on the completeness of the electrochemical discharge.

The introduction of zirconium to Ti–Ni alloys decreases the discharge capacity due to the formation of ZrNi and Zr_2Ni intermetallic compounds, which have very low discharge capacity because of the formation of hydride phases with strongly bound hydrogen states.[60] The capacity of $Ti_{0.8}Zr_{0.2}Ni_x$ alloys is considerably higher at $x > 1$. This may be due to the formation of a hydride phase based on Zr_7Ni_{10}, whose enthalpy of formation is lower than that of a hydride phase based on ZrNi. An increase in the zirconium content in the Ti–Zr–Ni alloy results in a noticeable increase in the cyclic stability, but a greater number of activation cycles is then required for attaining the appropriate discharge capacity.

6. Metal hydride electrodes based on multicomponent Laves phases

Titanium and zirconium do not form two-component Laves phases with nickel. These phases can exist only in ternary systems with partial substitution of nickel for other metals.[79]

Of two-component alloys with the AB_2 stoichiometry, ZrV_2, $ZrCr_2$, $ZrMn_2$, $TiCr_2$, and $TiMn_2$ have attracted most attention. They are characterised by the high stability of hydride phases that can be considerably decreased by replacing part of the zirconium by titanium and of the second metal by iron, cobalt, copper, nickel, or by addition of a hyperstoichiometric amount of a B-type element, or by a combination of these methods.

Alloys based on ZrV_2 with partial replacement of vanadium by nickel and of zirconium by titanium were first proposed for use in MH electrodes in a patent[16] and were then studied more thoroughly by several workers.[17,80] It was found that the content of vanadium and nickel should lie within the limits $Zr.V_{0.1-0.6}Ni_{1.9-1.4}$ in order to provide optimum discharge and cyclic characteristics. The high discharge capacity of hyperstoichiometric alloys of the composition $Zr(V_{0.33}Ni_{0.67})_{2.4}$ predetermined their choice as a base material for developing multicomponent MH electrodes with improved characteristics.[17] The replacement of 12.5% to 25% of the nickel by manganese results in an increase in the discharge capacity, which is ~370 mA h g^{-1} for the $Zr(V_{0.33}Ni_{0.50}Mn_{0.17})_{2.4}$ alloy. The partial replacement of zirconium by titanium decreases the discharge capacity, whereas the replacement of nickel by cobalt or iron somewhat increases the discharge capacity. The introduction of a small amount of aluminium to Zr–V–Ni alloys noticeably increases the cyclic stability of MH electrodes. For example, the $Zr(V_{0.33}Ni_{0.67})_{2.4}$ alloy loses ~43% of the original capacity after 100 charge–discharge cycles, whereas the $Zr(V_{0.33}Ni_{0.67})_{2.4}Al_x$ alloys, where $x = 0.05-0.1$, lose as little as 12–15%.

It has been shown[57] that the partial replacement of manganese by vanadium in multicomponent alloys based on a $ZrNi_{1.2}Mn_{0.6}Cr_{0.2}$ Laves phase considerably increases the discharge capacity: from 240 mA h g^{-1} for $ZrNi_{1.2}Mn_{0.6}Cr_{0.2}$ to 360 mA h g^{-1} for $ZrNi_{1.2}Mn_{0.3}Cr_{0.2}V_{0.3}$.

At present, the number of studies and patents dealing with MH electrodes based on multicomponent Laves phases of the AB_2 stoichiometry approaches that concerning multicomponent alloys of the AB_5 type based on lanthanum or the 'mischmetall' (see Table 1); this is a result not only of the acceptable exploitation characteristics of these materials but also of their lower cost.

7. Thin-film, nanocrystalline and amorphous MH electrodes

In the early 1990s, Adachi et al.[81] used flash evaporation-deposition of a $LaNi_5$ powder onto a support to synthesise a thin, highly porous film that was stable under conditions of repeated sorption-desorption of gaseous hydrogen but possessed poor adhesion and lower sorption capacity than the bulk alloy.

Later, denser thin $LaNi_5$ and $LaNi_{2.5}Co_{2.5}$ films were obtained by high-frequency spraying.[82,83] Depending on the nature of the target and support and on spraying conditions (beam power, spraying time and support temperature), the films were either amorphous or crystalline. In the authors' opinion, the absence of a plateau on the discharge curves in alkaline solutions suggested that the adsorption of hydrogen gave only a solid solution without the formation of a new hydride phase.

The discharge characteristics listed in Table 2 for MH electrodes of this type show that a decrease in the absorption capacity occurs on passing from bulk alloy to crystalline, and further to amorphous, film. This can be ascribed to the change in the distribution of crystallographic cavities suitable for hydrogen sorption and to an increase in the strength of the crystal lattice in thin films. The cyclic electrochemical stability of $LaNi_{2.5}Co_{2.5}$ films was found to be much higher than that of $LaNi_5$ films. The stability of films obtained in an atmosphere of hydrogen was higher than that of films obtained in argon, but their maximum capacity was twice as low because of the formation of a more stable protective layer on the surface.

Table 2. Discharge capacity and cyclic stability of powder and film MH electrodes.[83,84]

Form	C^0/mA h g^{-1}	$S(N)$ (%)
$LaNi_5$		
Powder	320	50 (160)
Crystalline film	160	50 (100)
	250[a]	40 (500)
Amorphous film	60	50 (15)
	160[a]	60 (500)
$LaNi_{2.5}Co_{2.5}$		
Powder	240	50 (400)
Crystalline film	120	75 (500)
Amorphous film	80	75 (200)

[a] Data from Ref. 84.

Thin-film $LaNi_5$ and $LaNi_{2.5}Co_{2.5}$ electrodes are highly active in the hydrogen evolution reaction, and the exchange currents on these electrodes are of the same order as those on the corresponding compact alloys ($\sim 10^{-4}$ A cm^{-2}).[83,84]

Crystalline and amorphous $LaNi_5$ films obtained by electron-beam evaporation of lanthanum and nickel in an ultrahigh vacuum[85] have higher capacity and cyclic stability than the films obtained by high-frequency spraying.[83]

It is unlikely that thin films would find practical use, at least in the near future. However, they are of particular interest in fundamental studies of hydrogen absorption by IMC and alloys.

It was reported recently that the structure of IMC affects the characteristics of MH electrodes.[23-25] It was found that, as in the case of thin-film electrodes, the amorphisation of the structure of a bulk alloy decreases the discharge capacity of the MH electrodes.[24] Of considerable interest are nanocrystalline IMC obtained by the fusion together of the components.[23,25] With $LaNi_5$, it was found[25] that these electrodes possess higher discharge capacity, lower equilibrium pressure of hydride dissociation and higher cyclic stability than macrocrystalline IMC. This effect of the size of the IMC particles on the characteristics of hydrogen absorption seems unexpected, since the solubility of hydrogen in Pd-electrodes has been found to decrease with increasing dispersity of Pd when particle sizes are $\leqslant 10$ nm.[86-89] When the palladium particles are smaller than 2.5 nm, hydrogen is no longer soluble in them.

IV. The technology of the manufacture and activation of metal hydride electrodes

The successful application of compact electrode materials requires their mechanical strength against destruction during charge-discharge and their corrosion stability in electrolyte solutions to be ensured. It is also necessary to solve the problems of electrical conductivity (the contact between the IMC grains), hydrophilicity (wetting) and porosity (accessibility of the whole bulk of an electrode material to the electrolyte). Various technological approaches are used to attain the necessary characteristics.

The mechanical destruction of electrodes due to hydrogen absorption–desorption is prevented by the use of binders, *viz.*, powders of metals (most often Cu, more rarely Ni and Co, and sometimes Au and Pt) or of polymeric organic compounds such as polytetrafluoroethylene (PTFE), polyethylene, polyvinyl alcohol, polystyrene, polyurethane, polyacrylic acid and silicones[47,90] or combinations of metal and polymeric powders.

The fraction of metal binder in electrode materials usually ranges from 60% to 80%. It has been found for a Cu binder[65] that increasing the mass ratio, alloy : binder, increases the internal resistance of the electrode material although the discharge characteristics remain almost unchanged.

The content of a polymeric binder is normally 15%–20%. Electron microscopic studies[14] of electrode materials containing polymeric binders showed that in these materials the IMC particles are enclosed in a three-dimensional framework, which, however, does not form a continuous and uniform film of the polymeric binder.

The introduction of acetylene black (up to 10%) is also recommended to improve the electric characteristics of electrode materials containing a polymeric binder,[46,48] and the hydrophilicity should be controlled by adding hydrophilisers.[46]

Electrode materials containing metal binders are activated more readily and have higher capacity and better charge–discharge reversibility[15,33] than electrodes with polymeric binders. However, in some cases the metal binder can be oxidised at electrode discharge potentials.

At present, a technological procedure of microcapsulation of the IMC particles with copper, nickel, cobalt, iron and palladium is widely used.[27,34,52,91-94] The metal coating (up to 20%) is applied by chemical or electrochemical deposition from solutions of the corresponding salts. A compact electrode material is then produced from the microcapsulated IMC powder with the addition of a polymeric binder (5%–10%). These electrodes have improved discharge characteristics and longer service life.[52,92]

It has been proposed[95] to cover the particles of IMC or a binder (coal, acetylene black) with a polymeric film by adsorption from a dilute emulsion of, for example, Teflon. The highest mechanical stability and cycling stability were shown by electrodes with 'teflonated' coal because an elastic, electrically conducting coal–Teflon framework provided a good contact between IMC grains.

A new method for modifying the surface of V–Ti alloys by sintering them with a nickel powder has been proposed.[96] The VNi_3 phase formed upon sintering is inert with respect to hydrogen, but catalytically affects hydrogen absorption–desorption in alkaline solutions and hence makes it possible to discharge an MH electrode.

All of the procedures for the manufacture of MH electrodes involve the introduction of additional components that decrease the specific capacity of an electrode material; hence, a decrease in the amount of a binder or the manufacture of binder-free electrodes are problems of current interest. In this respect, a noteworthy paper[97] reports the manufacture of electrodes that maintain their shape by the usual rolling of Zr–V–Ti–Ni–Cr alloys into the active compound without any binders or other additives, possibly due to unique physicochemical properties of these alloys.

Of particular interest are MH electrodes of amorphous alloys. They can be obtained in the form of a ribbon by very fast cooling of a melt and then used without any additional technological treatment.[47,61,98] However, it is still unclear, for how long the properties of such materials remain unchanged.

When working with MH electrodes, it is important to obtain as high a discharge capacity as possible for the IMC used. This goal is accomplished by activating the electrodes, that is, by repeating charge–discharge cycles, the number of which depends on many factors, primarily, on the IMC composition. However, in most cases the attainable discharge capacity of an MH electrode remains lower than the sorption capacity of the corresponding IMC from the gas phase, and in some cases, satisfactory discharge curves cannot be obtained at all (e.g., for $LaCo_5$,[84,99] $CeCo_3$,[14] YCo_3,[15] and V–Ti.[96]

The following processes occur during the activation of the electrode materials: (i) the alloy particles are dispersed during the absorption-desorption of hydrogen, hence a larger area of fresh, nonoxidized surface of the material is exposed to the electrolyte; (ii) the surface oxides are reduced, dissolved, or become electrically conducting; (iii) a catalytically active metal (e.g., nickel) is accumulated on the surface; (iv) the porosity of the structure increases and access of the electrolyte to an IMC surface becomes easier.

The latter phenomenon has been investigated in several studies[100,101] by the method of standard porosimetry of the electrode materials prepared from $CeNi_3$, $CeNi_2Co$ and ZrNi with a polymeric binder, using two measuring liquids, decane and water.

Fig. 2 presents the integral distribution curves of pore volume vs. their radii (porograms) in an initial electrode material based on ZrNi and PTFE and in the same material after prolonged cathodic polarisation in the region of hydrogen evolution. The total bulk porosity of a nonactivated Zr–Ni electrode is as low as $\sim$ 13% and is little affected by activation. (For example, activation increases the total bulk porosity of a $CeNi_3$ electrode (6%–8%) by a factor of 2.5–3.[100]) The volume of hydrophilic pores in a Zr-Ni sample is $\sim$ 50% of the total pore volume; mixed pores occupy a considerable volume (curve *2'*). The pore radii in the materials analysed varied from 10^2 to 10^4 nm and almost did not change during activation.

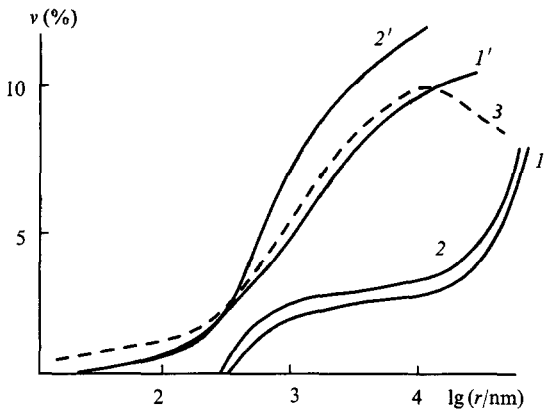


Figure 2. Integral distribution curves of pore volume *vs.* pore radius for a nonactivated (*1*, *1'*) and activated (*2*, *2'*, *3*) Zr–Ni electrode plotted by measuring the evaporation of water (*1*, *2*, *3*) and decane (*1'*, *2'*).[101]

Of particular interest in Fig. 2 is curve *3* obtained by measuring the evaporation of water from a Zr–Ni electrode immediately after cathodic polarisation without preliminary drying. In this case, the porosity is almost the same as that measured from decane evaporation. It is likely that during cathodic polarisation, a pressure drop arises in the bulk of the material due to intense liberation of hydrogen. As a result, the electrolyte fills even the hydrophobic pores, and this should increase the effective electrical conductivity of the material.

To decrease the number of activation cycles, IMC powders are sometimes pretreated with reducing reagents (H_3PO_2, KBH_4)[61,102] or with solutions of fluorides in order to convert the oxide layer into a fluoride layer.[31,103] An unexpected enhancement of the activity of Ti–Zr–V–Ni alloys was observed upon their oxidative treatment with oxygen or after anodic polarisation in an alkali.[17,104] This effect was explained by a change in the structure of the superficial zirconium oxide: a dense hydrogen-impermeable layer of a monoclinic modification of ZrO_2 is transformed into a tetragonal, hydrogen-permeable modification.

When Ti–Zr–V–Ni alloys are treated with a hot concentrated solution of alkali (6 M KOH or 10 M NaOH, 65–70 °C), activation occurs as a result of the modification of the surface layer (accumulation of nickel metal) and of the surface cracking due to the absorption of evolved hydrogen.[68]

The modification of the surface of MH electrodes with palladium and cobalt[91] facilitates activation by acceleration of the hydrogen discharge reaction, and the introduction of small amounts of rare-earth elements (La, Mm, Nd)[105] into ZrCrNi alloys facilitates activation due to the formation of a second, catalytically more active phase, or to a change in the structure of the surface layer.

V. Hydrogen evolution reaction on metal hydride electrodes

The cathodic polarisation of MH electrodes in electrolyte solutions results in the evolution of gaseous hydrogen along with the accumulation of dissolved hydrogen in the bulk of the electrode. The overall cathodic process includes the following steps.

1. Diffusion (convection) of the reacting species from the bulk of the solution to the electrode/solution interface

$$(H_2O)_b \rightleftarrows (H_2O)_s \text{ (alkaline solution).}$$

The 'b' index refers to the solution bulk, and 's' refers to the electrode/solution interface.

2. Charge transfer

$$(H_2O)_s + \bar{e} \rightleftarrows H_{ads} + (OH^-)_s \text{ (Volmer reaction).}$$

3. Diffusion of the reaction products from the surface of the electrode

$$(OH^-)_s \rightleftarrows (OH^-)_b, \quad H_{ads} \rightleftarrows H_{in},$$

where H_{in} indicates an intermediate position of H atoms directly below the superficial atomic layer of the metal (near-surface hydrogen).

4. Diffusion of hydrogen into the bulk of the IMC particles

$$H_{in} \rightleftarrows H^s_{abs},$$

$$H^s_{abs} \rightleftarrows H_{abs}(\alpha),$$

where $H_{abs}(\alpha)$ indicates hydrogen dissolved in the α-phase,

$$H_{abs}(\alpha) \rightleftarrows H_{abs}(\beta) \text{ (phase transition),}$$

$$2\,H_{abs}(\beta) \rightleftarrows H_2(\beta),$$

where $H_2(\beta)$ is hydrogen dissolved in the β-phase.

5. Desorption of adsorbed hydrogen

$$2\,H_{ads} \rightarrow H_2 \text{ (Tafel recombination reaction),}$$

$$H_{ads} + H_2O + \bar{e} \rightarrow H_2 + (OH^-)_s \text{ (Heyrovsky reaction).}$$

The problem of finding the slow step in such a complex process and determining the rates of separate steps is an independent current problem of electrochemical kinetics and electrocatalysis which still continues to attract attention.

The activity of MH electrodes in the hydrogen evolution reaction (HER) is mostly determined by the elemental composition of the IMC;[14,84,106–110] it also depends on the composition and properties of the electrode material as a whole (in particular, on the nature and amount of the binder[95,107]) and on the methods for the manufacture and pretreatment of MH electrodes.[108,111]

The observation of the low overvoltage of hydrogen evolution on TiNi and $LaNi_5$ was first made by Miles[112] and was confirmed in several studies,[84,106] in which the exchange currents of the HER on beads of the $LaNi_5$ and $LaCo_5$ alloys comparable to those for palladium[113] were observed. The synergistic effect on passing from pure metals to IMC was rationalised in terms of the sharply defined changes in the electronic properties of the alloys when lanthanum, containing *5d*-electrons, is introduced.

The electrocatalytic activity of the HER on various electrode materials prepared under similar conditions using Cu and PTFE as binders was the subject of several studies[14,107] (Table 3). The synergistic effect was not observed, i.e., electrodes based on $LaNi_5$ and Raney nickel had equal activity. The partial replacement of La by Mm and of Ni by Co decreased, while alloying the IMC with Ce increased, the activity of the electrode. The addition of Nb to $LaNi_5$ did not result in a noticeable enhancement of its electrocatalytic activity, whereas the addition of Nb to the TiFe alloy accelerated the HER by a factor of ~30.[110]

Table 3. Electrocatalytic activity of MH electrodes in the HER.[14,107]

IMC	Binder	$-\log(i_0/\text{A cm}^{-2})$
Ni	PTFE	5.0
$LaNi_5$	PTFE	5.0
$LaNi_5$	Cu	5.4
$La_{0.8}Ce_{0.2}Ni_2Co_3$	Cu	5.4
$La_{0.7}Nb_{0.3}Ni_{2.5}Co_{2.4}Cr_{0.1}$	Cu	5.8
$LaNi_{2.5}Co_{2.5}$	Cu	5.9
$MmNi_{3.5}Co_{0.7}Al_{0.8}$	Cu	5.9
$LaNi_{2.5}Co_{2.4}Mn_{0.1}$	Cu	6.1
$Mm_{0.5}La_{0.5}Ni_2Co_3$	Cu	6.1
$CeCo_3$	PTFE	4.6
$CeCo_2Ni$	PTFE	4.0
$CeCoNi_2$	PTFE	3.7
$CeNi_3$	PTFE	3.2

The activity of $CeNi_{3-x}Co_x$ electrodes increased[14] on increasing the Ni content of the alloy, and the exchange current density on $CeNi_3$ was found to be close to that on Pd.

The decrease in activity of $LaNi_5$ on passing from a PTFE binder to a Cu binder has not been rationalised.[107] This seems to be partially related to the difficulties in the determination of the actual electrode surface on which the HER occurs. For example, it was found for Ni electrodes prepared by different procedures[114] that hydrogen overvoltage is simultaneously affected by the inherent activity of the electrode material and by the change in the area of the real surface. To separate these effects it is necessary to compare the results obtained from polarisation curves and from impedance spectroscopy.

Hydrogen evolution on palladium, its alloys and hydrogen-sorbing materials occurs according to the Volmer–Tafel scheme. The overall overvoltage of the reaction (η) is a sum of overvoltages of the Volmer reaction (η_1) and the Tafel reaction (η_2) determined from the curves of decay (or rise) of potential after switching off (or on) the polarising current (η, t-curves). The kinetics of hydrogen evolution on palladium was considered taking several rate-determining steps into account,[115] which made it possible to describe completely the experimental polarisation $\eta, \log i$-curves.

Information on the mechanism and kinetics of the HER in alkaline solutions on $LaNi_5$ and Ti–Ni alloys was obtained using electrodes as thin amorphous films that are more stable mechanically during hydrogen sorption-desorption than the corresponding bulk alloys.[116] The results of quantitative processing of the η, t-curves presented in Table 4 showed that hydrogen evolution on $LaNi_5$ and Ti–Ni alloys occurs according to the Volmer–Tafel mechanism with comparable exchange currents of both steps. The slope of the straight regions on the $\eta, \log i$-curves was 120 mV, hence, at high η the overall reaction rate is determined by the charge transfer step. The exchange current ($i_{0,\mathrm{exp}}$) obtained by extrapolating the $\eta, \log i$-dependence to $\eta = 0$ differed from that obtained by the formula

$$\frac{1}{i_0} = \frac{1}{i_{0,\mathrm{V}}} + \frac{1}{i_{0,\mathrm{T}}},$$

where $i_{0,\mathrm{V}}$ and $i_{0,\mathrm{T}}$ are the exchange currents of the Volmer and Tafel reactions, respectively.

Table 4. Kinetic parameters of the HER on various cathodes in 1 M NaOH at 303 K.[116]

Sample	Thickness /Å	Exchange current density /μA cm^{-2}			
		$i_{0,\mathrm{V}}$	$i_{0,\mathrm{T}}$	i_0	$i_{0,\mathrm{exp}}$
$LaNi_5$	2000	3.22	0.70	0.58	1.7
	2000	3.86	0.68	0.57	
Ni	1000	—			1.4
Ni (wire)					0.45
$Ni_{0.11}Ti_{0.89}$	2000				2.1
$Ni_{0.5}Ti_{0.5}$	1500	2.46	0.93	0.67	1.7
$Ni_{0.76}Ti_{0.24}$	1500	2.76	0.15	0.81	2.6

It is evident from Table 4 that the $i_{0,\mathrm{exp}}$ values on thin-film alloys are similar to those on a nickel film and nickel wire as well as to the values previously obtained on amorphous NiTi.[117] Thus, the electrocatalytic activity of thin-film electrodes studied is determined by nickel, while synergism between lanthanum and nickel or titanium and nickel is not observed.

Results supporting the Volmer–Tafel mechanism for the hydrogen evolution reaction were also obtained for MH electrodes based on $LaNi_5$, $MmNi_5$, and $MmNi_{3.6}Mn_{0.4}Al_{0.3}Co_{0.7}$ powders.[99,118] The $i_{0,\mathrm{V}}/i_{0,\mathrm{T}}$ value is, for example, ~9 for the $MmNi_{3.6}Mn_{0.4}Al_{0.3}Co_{0.7}$ system, which suggests a mixed character for the rate-determining step. The addition of oxides such as Co_2O_4 or RuO_2 to an electrode material markedly accelerates the Volmer reaction and only slightly changes the rate of the Tafel reaction.

On the whole, however, the problem of the relation between the activity of IMC and its components with respect to the hydrogen evolution reaction cannot be regarded as completely solved. Solution of this problem requires the development of a procedure for the measurement and consideration of the real electrode surface area. On the other hand, the gradual change in the electronic properties of these materials on changing their composition affords a unique opportunity to reveal the fundamental problems of the nature of electrocatalytic activity.

VI. Charge-discharge processes on metal hydride electrodes

The electrochemical method of saturation of IMC with hydrogen requires much simpler equipment than that for saturation with gaseous hydrogen. However, electrochemical saturation at potentials corresponding to effective pressures above 0.098 MPa ($E_T < 0$ V) cannot be performed under equilibrium conditions due to concurrent hydrogen evolution. Thus, the effectiveness of MH electrode charging is determined by the ratio between the rates of hydrogen diffusion into the bulk of IMC particles and its desorption into the electrolyte bulk. The driving force of the sorption process is the difference between the chemical potentials of hydrogen on the surface, which is determined by the surface coverage by hydrogen, and in the bulk, which is determined by the overall fraction of occupied absorption sites.

Hydrogen sorbed by metals can exist in three different forms, namely, adsorbed hydrogen, hydrogen in a near-surface layer and dissolved hydrogen. An equilibrium is established between these forms. The quantity of near-surface hydrogen does not depend, while that of adsorbed hydrogen does depend, on the nature of the surface.[119] The sorption of hydrogen can be accompanied by phase transitions such as the formation of hydride phases (e.g. the $\alpha \rightleftarrows \beta$ transition in the case of the Pd electrode). No data are available on the type of isotherms of hydrogen electrochemical sorption on IMC, while the sorption isotherms on the Pd electrode differ in the α, $\alpha \rightleftarrows \beta$, and β regions.[1,120]

Under equilibrium conditions, the relation between the pressure of sorbed hydrogen (p_{H_2}) and the electrode potential is determined by the Nernst equation. At a cathodic polarisation, the dependence of p_{H_2} on η deviates from the Nernst equation and is determined by the mechanism of hydrogen evolution and the ratio of exchange currents of its different steps. In the case of the Volmer–Tafel mechanism, the relation between the hydrogen pressure at a certain polarisation ($\bar{p}$) and that at the equilibrium potential ($\bar{p}_0$) depends on the contribution of the overvoltage η_2 for the Tafel step by the equation[113]

$$\eta_2 = \frac{RT}{2F} \ln \frac{\bar{p}}{\bar{p}_0}.$$

It was found[108] that, after cathodic polarisation of a ZrNi electrode at potentials of hydrogen evolution followed by circuit disconnection, stationary potentials are established and maintained in the region from −0.04 to −0.008 V, depending on the polarisation potential and the composition of the solution. In addition, the passage from $\eta < -0.1$ to the −0.08 to −0.006 V range resulted in a considerable anodic current, which gradually decreased over a long period (hundreds of seconds), until converted into a cathodic current and attained the values corresponding to the rate of hydrogen evolution at the corresponding potential. An additional study showed that this does not result in dissolution of IMC components. The effects observed are evidently related to prolonged retention of hydrogen in the bulk of IMC due to hindrance of the recombination step or interphase transfer of hydrogen.[115,121]

The amount of the hydrogen sorbed can be determined by recording the discharge curves under galvanostatic conditions, i.e., by measuring the potential versus time at constant I, or under potentiostatic conditions, by measuring the current versus time at constant E.

The process of electrochemical discharge involves the following steps:

$$MH^{b}_{abs} \rightleftarrows MH^{s}_{abs}, \quad (3)$$

$$MH^{s}_{abs} \rightleftarrows MH_{ads}, \quad (4)$$

$$MH_{ads} + OH^{-} \rightleftarrows M + H_2O + \bar{e}, \quad (5)$$

Each of these can be the rate-determining step under certain conditions.

Metal hydride electrodes based on IMC and a binder are porous and differ considerably both from gas-diffusion porous electrodes[136,137] and from liquid-containing porous electrodes.[138] Gas-diffusion electrodes contain pores flooded with the electrolyte and gas-filled pores, through which the gaseous reagent is transported into the bulk of the electrode to the active catalyst surface. Porous electrodes made of hydrogen-sorbing IMC do not require gas porosity. These electrodes differ from liquid-containing electrodes by the continuous supply of the reagent by diffusion from inside material particles to their outer surfaces where the electrochemical reaction occurs. Thus, porous MH electrodes should be regarded as systems with parameters distributed over the electrode thickness and over the IMC particle radius (Fig. 3).

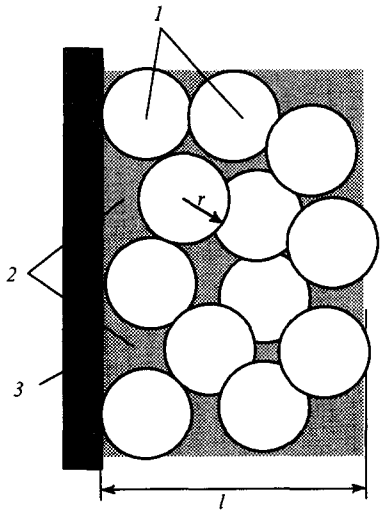


Figure 3. A model of a porous hydrogen-sorbing electrode:[126] (*1*) IMC particles; (*2*) solution-containing pores; (*3*) metal current collector; (*l*) electrode thickness; (*r*) radius of an IMC particle.

Several mathematical models have been suggested for the description of experimental discharge curves. These models can be divided into two groups: in one group, the models consider hydrogen diffusion only within IMC particles (along the radius r, see Fig. 3),[31,122-125] while in the other, models also take into account diffusion across the electrode thickness (along the coordinate l).[126,127]

Pshenichnikov and co-workers[122,123] proposed a model for calculating galvanostatic charge-discharge curves on an isolated spherical grain of a hydrogen-absorbing metal. Assuming that potential E is a single-valued function of the degree of surface coverage by adsorbed hydrogen, which is related to the hydrogen concentration in the bulk by the Frumkin isotherm, the authors took the nonstationary mass transfer in a unit grain into account and obtained a relation between E and the amount of electricity

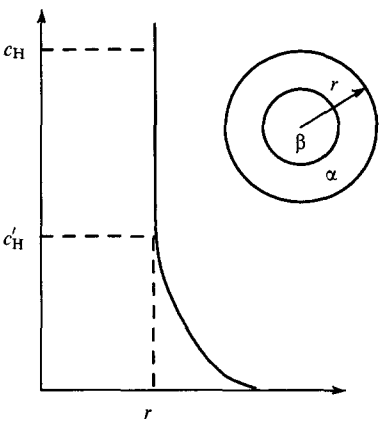


Figure 4. A scheme for the variation of the hydrogen concentration in a spherical particle during discharge:[31] (c_H) hydrogen concentration in the β-phase; (c'_H) hydrogen concentration at the interface between the α- and β-phases.

passed. By adjusting the adsorption equilibrium constant within this model, they managed to obtain qualitative agreement between the experimental and calculated data. If one assumes that the electrode consists of particles with two different radii, charge-discharge curves with two delays can be obtained. Based on this model, it was concluded that the total charging and discharging of a grain are impossible if the diffusion current is commensurate with the charging current.

It was believed[31,124] that the quantity of ionised hydrogen is proportional to the thickness of the surface α-layer (Fig. 4) and that the rate of discharge at low discharge currents is determined by hydrogen diffusion in the α-phase. Under these conditions, the dependence of the discharge capacity (C) on the discharge current (I) has the following form:

$$C = C^0\left\{1 - \left(1 + \frac{C^0 k_5}{I}\right)^{-3}\right\},$$

where C^0 is the discharge capacity (at $I \to 0$) and k_5 is the rate constant of the discharge step (5).

At high discharge currents, the rate-determining step is the electrochemical reaction occurring on the Ni-centres

$$H(atom) + H_2O = H_3O^{+} + \bar{e}, \quad (6)$$

and the dependence of the discharge capacity on the discharge current acquires the form

$$C = C^0\left\{1 - \exp\left[-k_6\left(\frac{C}{I}\right)^n\right]\right\}, \quad (7)$$

where n is an empirical constant and k_6 is the rate constant of reaction (6).

The model proposed was tested for a $LaNi_{4.7}Al_{0.3}$ electrode. The dependences of $\log\log[1/(1 - C/C^0)]$ on $\log(C/I)$ contained a break point at currents of ca. 1000 mA g^{-1}, which indicated a change in the discharge mechanism. The experimentally determined discharge capacities coincided with those calculated by equation (7); the k_6 value depended on the duration of the treatment of the electrode surface with a potassium fluoride solution due to changes in the composition of the surface layer.

The basic feature of yet another model[125] is the possibility of quantitative processing of step (4) as a heterogeneous chemical reaction. The authors derived equations for hydrogen diffusion in the bulk of electrodes of various shapes (plate, cylinder, sphere), which coincide with the equations obtained previously by Bucur et al.[128,129] who theoretically described the ionisation of hydrogen dissolved in a Pd electrode. The concentration of hydrogen in the

near-surface layer (c_H^s) at low D/l^2 (where D is the diffusion coefficient of hydrogen and l is a parameter determined by the electrode size) and low discharge currents decreases linearly with increase in the discharge time (t). At high D/l^2 and/or higher discharge currents, the c_H^s value linearly depends on t only within a narrow time range. In this case, when c_H^s reaches zero (i.e., the discharge is effectively finished), the bulk of the electrode still contains a fraction (f) of the dissolved hydrogen that cannot be ionised because of the limited rate of hydrogen diffusion. The value

$$f \cong \frac{Il}{c^0 D}$$

(where c^0 is the initial concentration of the dissolved hydrogen) characterises the effectiveness of discharge. It depends on the electrode geometry and decreases in the series: plate > cylinder > sphere.

Based on the theoretically derived equation for the dependence of the electrode potential on t under galvanostatic discharge conditions, experimental discharge curves for MH electrodes made of $ZrNi_2$, $Zr(V_{0.33}Ni_{0.67})_{2.4}$ and $Zr(CrFe)_2$ were analysed and the kinetic parameters of steps (3) – (5) were calculated. They were found to depend not only on the electrode composition but also on the surface structure or the phase composition of the hydride phase.

The discharge capacity at low discharge currents is obtained by subtracting two quantities linearly dependent on the current, the first one being related to the liming rate of hydrogen diffusion in the electrode bulk and the other to the limiting rate of hydrogen transfer from the absorbed to the adsorbed state, from the equilibrium capacity C,

$$C = C^0 - \frac{Il}{aD} - C_0 \frac{I}{Fk_4 c_H^0},$$

where a is a constant depending on the electrode geometry, and k_4 is the rate constant of reaction (4). Thus, the linear C,I dependences observed at low discharge currents are analogous to those found in a previous study.[128]

At high discharge currents

$$C = (C^0)^2 \frac{\pi D}{bISl^2}\left(1 - \frac{ISl}{cFk_4 c_H^0}\right)^2$$

where b and c are constants depending on the electrode geometry, and S is the surface area of the electrode.

The model described above is applicable only when the chemical potential of hydrogen (μ_H) changes continuously with changes in the concentration (c_H) in the bulk of the electrode; in particular, this is the case for amorphous films. In the case of crystalline alloys, for which the μ_H, c_H-dependences contain a plateau due to a phase transition, the model describes only single-phase regions (the starting and terminal regions) of the discharge curves.

Models based on the macrokinetics of the ionisation of the dissolved hydrogen in porous MH electrodes have also been proposed.

A theory was proposed[126] that considered a porous planar electrode of thickness l consisting of spherical IMC particles of radius r. The joint application Fick's second law and theories of slow discharge and charge-discharge of the electric double layer gave a system of equations with four dimensionless parameters determined by the characteristic times of the following processes: hydrogen diffusion in a particle; charging of the electric double layer of a porous electrode; charging of the electric double layer of a smooth electrode; and reactions of hydrogen ionisation. In the general case, an analytical solution of this system is difficult; however, numeric modelling is possible by variation of three parameters: the diffusion coefficient of hydrogen, the capacity of the electric double layer and the exchange current density. By choice of the parameters, one can obtain the distribution of hydrogen concentration in the bulk of the particle and across the electrode thickness. When diffusion limitations prevail over ohmic limitations, the hydrogen distribution in the bulk of the electrode should play the major role. This dependence can be obtained by analytical methods.

A model was proposed[126] for the description of the discharge process by comparing the calculated and experimental potentiostatic discharge curves for an MH electrode compressed from a $CeNi_3$ powder with 20% PTFE. This model is applicable to any systems containing a phase of a reducible or oxidisable component; in particular, it was used for describing the charge – discharge behaviour of porous polyaniline electrodes under galvanostatic conditions.[130]

The following drawbacks of the model proposed by Vol'fkovich et al.[126] should be noted: first, electrode charging is complicated by a phase transition, which can be taken into account formally only by varying the double layer capacity; second, the step of interphase transfer of hydrogen (4) is not taken into account.

Another treatment of porous systems has been proposed[127] for a cylindrical electrode consisting of spherical IMC particles. The model takes into account the diffusion of hydrogen in the bulk of IMC particles (based on Fick's second law), the charge transfer and the potential drop in the IMC particles and in the electrolyte that fills the pores. For the majority of metals the potential drop in the metal phase is low: cycling of the electrode can decrease the electrical conductivity of the powder, e.g. due to the oxidation of the surface or impairment of contacts between the particles. Because the equations obtained[127] are very complex and the model uses a great number of parameters, it is difficult to apply this model to the analysis of experimental discharge curves. Furthermore, it does not permit calculation of the kinetic parameters of reactions (3) – (5).

Thus, none of the mathematical models proposed for describing the discharge process is general, since they do not take into account all the steps of the process. The models assume that the diffusion coefficient of hydrogen (D) does not depend on its concentration in the alloy, whereas the existence of this dependence has been established experimentally.[131, 132] In addition, the models proposed do not take into account the specific nature of the $\alpha \rightleftarrows \beta$ transition, except for the formal introduction of an infinitely large capacity corresponding to this transition.[126]

VII. Corrosion of metal hydride electrodes

One of the main properties of MH electrodes required for their practical application is a sufficiently high stability during repeated electrochemical charge – discharge cycles in electrolyte solutions. As has been noted, the measure of the cyclic stability is the $S(N)$ value, which is primarily determined by the nature of the IMC and the binder, the manufacturing method, and the pretreatment of the electrode.

The high stability of AB_5 type IMC containing Al, Si, Ti and Zr is determined by a superficial oxide film formed during electrode cycling in alkaline solutions.[13, 29, 34, 37, 117, 133, 134]

The addition of manganese to alloys, often used for decreasing the hydride dissociation pressure, impairs the corrosion stability of IMC. This is caused by the diffusion of manganese from the bulk to the surface and degradation of the alloy to give hydroxides of manganese and rare-earth elements as well as metallic nickel.[27, 33]

The increase in the plasticity of alloys on alloying $LaNi_5$ with Co decreases the rate of its dispersal and, as a consequence, decreases the newly formed surface prone to oxidation, imparting high stability to the alloy during cycling.[135 – 138]

It has been shown that the corrosion stability of the intermetallic compound $LaNi_{4.5}Mn_{0.5}$ produced under diverse conditions is affected by the disruption of the atomic order within the same AB_5 crystalline system: homogenisation of the structure increases the stability of the material.[30]

The effect of homogenising annealing or rapid cooling on the cyclic stability of $MmNi_{3.5}Co_{0.7}Al_{0.8}$ is explained[43] by the difference in size of IMC grains formed (~50 μm in the former case and ~10 μm in the latter), assuming that a protective oxide layer can be formed not only on the particle surface, but also at the grain boundaries. In the case of the quenched alloy, the cyclic stability was found experimentally to increase with decreasing grain size.

The spectrophotometric analysis of 1 M NaOH solutions after prolonged potentiostatic polarisation of YNi_3 and YCo_3 electrodes in these solutions showed[15] that the rate of yttrium dissolution from the IMC is lower by at least an order of magnitude than that from the pure metal, even at potentials much higher than the potential of the anodic boundary for total IMC dehydrogenation. Nickel and cobalt were found not to pass into solution over the whole range of potentials studied.

When an IMC of an AB_x type contacts an electrolyte, corrosion can be represented as follows:

$$AB_x + H_2O \overset{k_{ox}}{\rightleftharpoons} A(OH)_3 + xB\,[\text{or } BO, B(OH)_2] + H_2. \quad (9)$$

As a result of this heterogeneous reaction, the amount of the hydrogen-sorbing compound decreases in proportion to the specific surface. Thus, the larger the IMC particles, the weaker should be the trend to decreasing capacity. The validity of this hypothesis was confirmed for $LaNi_{4.4}Cu$ electrodes produced from powders with different specific surfaces.[22]

As follows from the above considerations, the disintegration of IMC grains into smaller particles during the charge-discharge process stimulates corrosion. The comminution of IMC grains is caused by the coexistence of various hydrides on the surface. These hydrides increase the volume of the unit cell to different extents; as a result, mechanical stress appears at the boundaries of hydride grains, leading to brittleness of the system and to increased local mobility of metal atoms contained in the IMC.[13,29]

These concepts were further developed in a study of the effect of electrode cycling on: the in situ X-ray diffraction spectra; the hydrogen concentration; the variation of the unit cell volume upon formation of α- and β-phases ($V_\beta - V_\alpha$); the variation of the overall unit cell volume upon hydride formation ($V - V_0$); and the electrode stability (Table 5).[19]

The ($V_\beta - V_\alpha$) and ($V - V_0$) values for the $LaNi_x$ and $LaNi_{x-1}Cu$ electrodes decrease with an increase in the non-stoichiometry of a system, the ($V_\beta - V_\alpha$) value decreasing much more quickly. The introduction of copper into the alloy primarily affects the ($V_\beta - V_\alpha$) value. The stability of the alloys is determined by the changes in the volume of the unit cell upon formation of the β- and α-phases. An increase in ($V_\beta - V_\alpha$) enhances mechanical strain and the desintegration of the alloy particles in agreement with the results of microscopic studies.

A mathematical model of the degradation of MH electrodes has been developed[22] based on the assumption that the specific surface is the main factor determining the rate of particle oxidation.

Table 5. Stability of MH electrodes and changes in unit cell volume upon hydride formation.[19]

Alloy	AB_x	$(V_\beta - V_\alpha)/V_0$ (%)	$(V - V_0)/V_0$ (%)	$S(400)$, (%)
$LaNi_5$	AB_5	21.5	22.5	15
$LaNi_{5.4}$	$AB_{5.4}$	19.9	22.0	25
$LaNi_4Cu$	AB_5	17.0	21.2	16
$LaNi_{4.2}Cu$	$AB_{5.2}$	13.2	19.7	62
$LaNi_{4.4}Cu$	$AB_{5.4}$	2.8	18.2	90
$LaNi_5Cu$	AB_6	0.0	8.5	98

For spherical particles with initial radii r_0, the electrode capacity after cycling for a period t is

$$C_t^{1/3} = C_t(0)^{1/3} - l\,[\tfrac{1}{3}C_t(0)^{1/3}S_0k_9a_{H_2O}M_{AB_x}]t \quad (10)$$

where $C_t(0)$ is the electrode capacity before cycling, S_0 is the initial specific surface of the powder, a_{H_2O} is the activity of water, M_{AB_x} is the IMC mass, and k_9 is the rate constant of reaction (9). If the diffusion of the water molecules is not the rate-determining step, then a linear dependence of $C_t^{1/3}$ on t should be observed. Such dependence was obtained for $LaNi_{4.4}Cu$ electrodes with three different S_0 values.[22] The increase in the slope of the straight lines correlated well with the size of the alloy particles. All three straight lines intersected at one point but not at $t = 0$.

Equation (10) can be transformed into

$$C_t = C_t(0)\exp(-S_0k_9a_{H_2O}M_{AB_x}t)\,. \quad (11)$$

Since $t = bN$, where b is a proportionality factor, relation (11) is analogous to the empirical equation[13]

$$C(N) = C_0\exp\left(-\frac{N}{N^*}\right), \quad (12)$$

where C_0 is the maximum capacity, $C(N)$ is the capacity in the Nth cycle, and parameter N^* reflects the rate of capacity decrease and is regarded as a stability constant. It follows from equations (11) and (12) that

$$N^* = \frac{1}{S_0k_9M_{AB_x}}\,.$$

One of the drawbacks of the model is that it does not account for the dependence of the oxidation rate on the surface state (oxidised or reduced) and on the potential. In addition, cycling gradually changes the composition of the surface layer and, hence, its protective properties.

A model including the changing discharge capacity of MH electrodes caused during cycling proposed in another study[31] simultaneously accounts for the discharge and degradation processes. During low-current cycling, the decrease in the capacity over time should obey the following equation:

$$C(I,N) = C(0,0)\left\{1 - \left[1 + \frac{C(0,0)k_1}{I}\right]^{-3}\right\}\times$$
$$\times[1 - P\exp(-FN)]\exp(-K_NN)\,, \quad (13)$$

while during high-current cycling, the following equation is obeyed:

$$C(I,N) = C(I,0)[1 - P\exp(-kN)\exp(-k_1N)]$$
$$C(I,0) = C(0,0)\left\{1 - \exp\left[-\frac{v_1C(I,0)^n}{I^n}\right]\right\}, \quad (14)$$

where $C(0,0)$ is the capacity at the zeroth cycle, I is the discharge current, N is the number of galvanostatic cycles, k_1 is the rate constant of the electrochemical discharge reaction, P is the fraction of the hydrogenated alloy particles active in the cycling, k is the rate constant of the MH electrode activation, K_N is the factor of degradation of the capacity of the MH electrode equal to $S_cLy^2\Delta t$ (S_c is the fraction of corroded specific surface, L is the number of hydride particles per unit area, y is the rate of hydride growth, and Δt is the time of corrosion during each charge-discharge cycle), v_1 is the rate of the electrochemical reaction, and n is an empirical constant.

The dependence of the discharge capacity of untreated and fluoride-treated $LaNi_{4.7}Al_{0.3}$ electrodes on the discharge current and the number of cycles were plotted, the constants were calculated by use of equations (13) and (14), and three-dimensional C,I,N-diagrams were plotted.[31] The dependence of kinetic and corrosion characteristics on the time of treatment of

the electrodes with fluoride ions was explained by the following reactions:

$$La(OH)_3 + 3F^- = LaF_3 + 3OH^-;$$

$$LaNi_{4.7}Al_{0.3} + 0.6K^+ + 4.5F^- =$$

$$= LaF_3 + 0.3K_2AlF_5 + 4.7Ni^0 \text{ (or } Ni^{2+}),$$

leading to the accumulation of catalytically active nickel and of LaF_3, which has better protective properties than $La(OH)_3$, on the surface.

Up to the present, almost no systematic data are available on the cyclic stability of AB_3-type IMC, where A is Ce or Y, and B is Ni or Co. For MH electrodes based on multicomponent Laves phases, only the results of electrochemical charge–discharge cycling tests have been reported (see Table 1). However, the mechanism and the nature of the accompanying degradation processes have not been considered, although, because of the different elemental composition, they would probably differ from those in the rather well-studied IMC of AB_5 type and their substituted derivatives.[139–148]

VIII. Conclusion

To date, several countries have set up the production of nickel–metal hydride accumulators. For example, the number of such accumulators in Japan is as high as 25% of the number of nickel–cadmium current sources, and there exists a trend for a gradual displacement of the latter. This is caused both by environmental considerations and by the good specific characteristics of MH-accumulators as well as by the possibility of manufacturing them without considerable investment and with almost the same equipment. Along with small-scale MH-accumulators for portable computers, video cameras and home electronic appliances, large MH-accumulators are being developed, in particular, for electric cars.

As has been shown above, the properties of hydride-forming materials depend very strongly on their composition and change considerably on adding apparently insignificant quantities of several elements or on small changes in stoichiometry. For example, the addition of less than 2 at.% Li[149] or a decrease in the stoichiometric coefficient to 4.5–4.8[147] increases the capacity of the $Mm(NiCoAlMn)_5$ electrode with respect to hydrogen, and the service life of the MH battery reaches 1000 cycles with loss of less than 10% of the initial capacity. Therefore, the problem of optimising the composition of hydride electrodes is still of current interest. From the fundamental scientific aspect, a theoretical analysis of the effect of the composition and of concentrations of particular components on the sorption properties of IMC is required. Some approaches to the problem have been reported; however, they have not been developed and generalised because primary attention was paid to extensive empirical studies aiming at the solution of applied problems.

The facts set forth above suggest that active electrochemical investigations of hydride-forming IMC have in fact led to the appearance of a new field, i.e., electrochemistry of hydrides. The particular features of these materials are the strong dependence of their properties on the amount of hydrogen sorbed and their specific electrochemical behaviour. Unfortunately, the latter has been studied insufficiently, although, judging by certain theoretical considerations and preliminary data, one can anticipate that these materials would have unusually high electrocatalytic activity and selectivity in electrochemical hydrogenation and reduction.[78, 111, 140–142]

A detailed study of the pronounced degradation processes occuring upon hydrogen sorption can lead to a deeper insight into the nature of hydrogen embrittlement of materials, which is particularly important for the prediction of the corrosion behaviour of certain metals and alloys, for hydride materials science and electrochemical technology. Possibly cheap hydrogen-sorbing materials will be found in the future and used as gas-separating membranes in various systems, including electrochemical ones. As yet, such membranes are most frequently made of palladium and its alloys. It has been found that when palladium is alloyed with rare-earth metals its properties as a membrane are improved.[143, 144] It is not known at present whether similar membranes can be created using the typical IMC representatives considered above. The realisation of this possibility would drastically expand the field of use of hydrogen-sorbing IMC.

Intermetallic compounds sorbing hydrogen are interesting and promising subjects for revealing the nature of fine interactions in hydride phases. These investigations performed over a broad temperature range and using deuterium as a sorbate[145, 146] show the most promise. It can be expected that investigations in this field will lead to the appearance of new concepts in hydride chemistry.

References

1. G Alefeld, J Völkl (Eds) *Hydrogen in Metals* Vol. 2 (Berlin: Springer, 1978)
2. T V Gel'd, R A Ryabov, L P Mokhracheva *Vodorod i Fizicheskie Svoistva Metallov i Splavov* (Hydrogen and Physical Properties of Metals and Alloys) (Moscow: Nauka, 1982)
3. P Nylen *Z. Elektrochem.* **43** 915 (1937)
4. A N Frumkin, in *Advances in Electrochemistry and Electrochemical Engineering* Vol. 3 (Ed. P Delahay) (New York: Interscience, 1963) p. 287
5. A N Frumkin, N A Alajalova *Acta Physicochim. USSR* **18** 1 (1944)
6. E W Justi, H H Ewe, A W Kalberlah, N M Saridakis, M H Schaefer *Energy Convers.* **10** 183 (1970)
7. M A Gutjahr, H Buchner, K D Beccu, H Saufferer, in *Power Sources* Vol. 4 (Ed. D H Collins) (Newcastle upon Tyne: Oriel Press, 1973) p. 79
8. H H Ewe, E W Justi, K Stephan *Energy Convers.* **13** 109 (1973)
9. US P. 3 874 928; *Ref. Zh. Khim.* 5 L 327P (1976)
10. A Percheron-Guegan, F Briaucourt, H Diaz, J C Achard, J Sarradin, G Bronoel, in *The 12th Rare Earth Research Conference (Proceedings)* (Ed. C E Lundin) (Denver, CO: Univ. Denver, 1976) p. 300
11. A Percheron-Guegan, J C Achard, J Sarradin, G Bronoel, in *Hydrides for Energy Storage* (Eds A F Andresen, A J Maeland) (Oxford: Pergamon Press, 1978) p. 485
12. M H J Van Rijswick in *Hydrides for Energy Storage* (Eds A F Andresen, A J Maeland) (Oxford: Pergamon Press, 1978) p. 261
13. J J G Willems *Philips J. Res.* **39** 1 (1984)
14. O A Petrii, K N Semenenko, I I Korobov, S Ya Vasina, I V Kovrigina, V V Burnasheva *J. Less-Common Met.* **136** 121 (1987)
15. I I Korobov, S Ya Vasina, O A Petrii, G A Tsirlina, M Yu Rusanova *Elektrokhimiya* **31** 652 (1995)
16. US P. 4 551 400; *Chem. Abstr.* **104** 53 682w (1988)
17. S Wakao, H Sawa, J J Furukawa *J. Less-Common Met.* **172–174** 1219 (1991)
18. P H L Notten, R E F Einerhand *Adv. Mater.* **3** 343 (1991)
19. P H L Notten, R E F Einerhand, J L C Daams *J. Alloys Compd.* **210** 221; 233 (1994)
20. X Gao, D Song, Z Zhou, H Yang, Y Zhang, P Shen, in *The International Symposium on Metal–Hydrogen Systems (Abstracts of Reports)* (Fujiyoshida, Japan, 1994) Mo.B7
21. H Sawa, S Wakao, J Furukawa *Denki Kagaku* **59** 945 (1991)
22. S-R Kim, J Y Lee *J. Alloys Compd.* **210** 109 (1994)
23. L Varga, A Lovas, K Tompa, J Joubert, A Percheron-Guegan, in *The International Symposium on Metal–Hydrogen Systems (Abstracts of Reports)* (Fujiyoshida, Japan, 1994) Fr.A1
24. H Miyamura, T Sakai, N Kuriyama, I Uehara, N Shiraishi, T Iwasaki, in *The International Symposium on Metal–Hydrogen Systems (Abstracts of Reports)* (Fujiyoshida, Japan, 1994) Mo.P40
25. Z Chen, M Lü, Z Hu, in *The International Symposium on Metal–Hydrogen Systems (Abstracts of Reports)* (Fujiyoshida, Japan, 1994) Th.B7
26. W Hu, Y Zhang, D Song, J Huag, Y Wang, X Gao, in *The International Symposium on Metal–Hydrogen Systems (Abstracts of Reports)* (Fujiyoshida, Japan, 1994) Mo.P21

27. T Sakai, K Oguro, H Miyamura, N Kuriyama, A Kato, H Ishikawa *J. Less-Common Met.* **161** 193 (1990)
28. S Wakao, Y Yonemura *J. Less-Common Met.* **89** 481 (1983)
29. J J G Willems, K H J Buschow *J. Less-Common Met.* **129** 13 (1987)
30. W Tang, G Sun *J. Alloys Compd.* **203** 195 (1994)
31. Z Li, D Yan, S Suda *Res. Rep. of Kagakuin Univ.* **75** 113 (1993)
32. T Sakai, H Ishikawa K Oguro, C Iwakura *Prog. Batt. Solar Cells* **6** 221 (1987)
33. S Ya Vasina, Kh M Shao, I I Korobov, O A Petrii *Elektrokhimiya* **32** (1996) (in the press)
34. T Sakai, H Miyamura, N Kuriyama, A Kato, K Oguro, H Ishikawa *J. Less-Common Met.* **159** 127 (1990)
35. F Meli, A Züttel, L Schlapbach, in *The International Symposium on Metal–Hydrogen Systems (Abstracts of Reports)* (Fujiyoshida, Japan, 1994) Tu.B4
36. F Meli, A Züttel, L Schlapbach *J. Alloys Compd.* **190** 17 (1992); **202** 81 (1993)
37. T Sakai, H Miyamura, N Kuriyama, A Kato, K Oguro, H Ishikawa *J. Electrochem. Soc.* **137** 795 (1990)
38. T Sakai, H Miyamura, K Oguro, A Kato, H Kuriyama, H Ishikawa *Denki Kagaku* **57** 612 (1989)
39. D C Magnuson, H F Gibbres *Mater. Lett.* **21** 1 (1994)
40. C Folonari, F Iemmi, F Manfredi, A Rolle *J. Less-Common Met.* **74** 371 (1980)
41. Z-P Li, Y-Q Lei, C-P Chen, J Wu, Q-D Wang *J. Less-Common Met.* **172–174** 1265 (1991)
42. M Ohnishi, Y Matsumura, K Hasegawa, M Oshitani, K Takeshima *Yuasa Yiho* **75** 4 (1993)
43. T Sakai, T Hazama, H Miyamura, N Kuriyama, A Kato, H Ishikawa *J. Less-Common Met.* **172–174** 172; 1175 (1991)
44. T Hara, N Yasucha, Y Takeuchi, T Sakai, A Uchiyama *J. Electrochem. Soc.* **140** 2450 (1993)
45. T Sakai, H Yashinaga, H Miyamura, N Kuriyama, H Ishikawa *J. Alloys Compd.* **180** 37 (1992)
46. M Yamashita, H Higuchi, H Takemura, K Okuno *Denki Kagaku* **61** 729 (1993)
47. J Choi, C-N Park *J. Alloys Compd.* **217** 25 (1995)
48. M Kanda, M Yamamoto, K Kanno, Y Satoh, H Hayashida, M Suzuki *J. Less-Common Met.* **172–174** 1227 (1991)
49. K Hasegawa, H Mori, M Oshitani *Yuasa Yiho* **71** 13 (1991)
50. Jpn. P. 62/119 863 [871 119 863]; *Chem. Abstr.* **107** 99 770p (1987)
51. Jpn. P. 61/168 871 [86 168 871]; *Chem. Abstr.* **106** 7 556b (1987)
52. M Geng *J. Alloys Compd.* **206** L.3 (1994)
53. Jpn P. 62/119 864 [87 119 864]; *Chem. Abstr.* **107** 99 769v (1987)
54. Jpn. P. 61/214 361 [86 214 361]; *Chem. Abstr.* **106** 105 440d (1987)
55. Jpn. P. 61/233 969 [86 233 969]; *Chem. Abstr.* **106** 87 709s (1987)
56. L Jiang, F Zhan, D Bao, G Ging, Y Li, X Wei, in *The International Symposium on Metal–Hydrogen Systems (Abstracts of Reports)* (Fujiyoshida, Japan, 1994) Mo.P22
57. Y Moriwaki, T Gamo, H Seri, T Iwaki *J. Less-Common Met.* **172–174** 1211 (1991)
58. M Sugawara, T Endo, K Matsuki *Denki Kagaku* **57** 488 (1989)
59. H Sawa, S Wakao, J Furukawa *Denki Kagaku* **58** 862 (1990)
60. S Wakao, Y Yonemura, H Nakano, H Shimada *J. Less-Common Met.* **104** 365 (1984)
61. M Matsuoka, K Asai, K Asai, Y Fukumoto, C Iwakura *J. Alloys Compd.* **192** 149 (1993)
62. H Sawa, K Ohzeki, M Ohta, H Nakao, S Wakao *Z. Phys. Chem. N.F.* **164** 1521 (1989)
63. A Züttel, F Meli, L Schlapbach *J. Alloys Compd.* **203** 235 (1994)
64. M Tsukahara, K Takahashi, T Mishima, H Miyamura, N Kuriyama, T Sakai, I Uehara, in *The International Symposium on Metal–Hydrogen Systems (Abstracts of Reports)* (Fujiyoshida, Japan, 1994) We.B5
65. A Züttel, F Meli, L Schlapbach *J. Alloys Compd.* **206** 31 (1994)
66. US P. 4 849 205; *Chem. Abstr.* **111** 8 1436g (1989)
67. D Song, X Gao, Y Zhang, J Yan, P Shen *J. Alloys Compd.* **206** 43 (1994)
68. D-Y Yan, G Sandrock, S Suda, in *The International Symposium on Metal–Hydrogen Systems (Abstracts of Reports)* (Fujiyoshida, Japan, 1994) Mo.P43; *J. Alloys Compd.* **216** 237 (1994)
69. H Miyamura, N Kuriyama, T Sakai, K Oguro, A Kato, H Ishikawa, T Iwasaki *J. Less-Common Met.* **172–174** 1205 (1991)
70. T Sakai, A Takagi, T Hasama, H Miyamura, N Kuriyama, H Ishikawa, C Iwakura, in *The III International Conference on Batteries for Utility Energy Storage (Proceedings)* (Kobe, Japan, 1991) p. 499
71. C Iwakura, M Matsuoka *Prog. Batt. Solar Cells* **10** 81 (1991)
72. P H L Notten, P Hokkeling, in *The 178th Electrochemical Society Meeting (Ext. Abstracts)* (Seattle, USA, 1990) No. 75
73. P H L Notten, J L C Daams, R E F Einerhand *Ber. Bunsenges Phys. Chem.* **96** 656 (1992)
74. P H L Notten, P Hokkeling *J. Electrochem. Soc.* **138** 1877 (1991)
75. M M Jaksic *High Temp. Sci.* **30** 19 (1990)
76. K N Semenenko, O A Petrii, S Ya Vasina, I I Korobov, I V Kovrigina *Dokl. Akad. Nauk SSSR* **276** 1424 (1984)
77. I V Kovrigina, S Ya Vasina, I I Korobov, O A Petrii, K N Semenenko *Elektrokhimiya* **22** 1143 (1986)
78. O A Petrii, I V Kovrigina, S Ya Vasina *Mater. Chem. Phys.* **22** 51 (1989)
79. D G Ivey, D O Northwood *Z. Phys. Chem. N.F.* **147** 191 (1986)
80. US P. 4 728 586; *Chem. Abstr.* **109** 76 599s (1988)
81. G Adachi, K Niki, J Shiokawa *J. Less-Common Met.* **81** 345 (1981)
82. T Sakai, H Miyamura, K Oguro, T Iwasaki, H Ishikawa *Z. Phys. Chem. N.F.* **164** 1539 (1989)
83. T Sakai, H Ishikawa, H Miyamura, N Kuriyama, S Yamada, T Iwasaki *J. Electrochem. Soc.* **138** 908 (1991)
84. H Tamura, C Iwakura, T Kitamura *J. Less-Common Met.* **89** 567 (1983)
85. Y Li, Y-T Cheng, M A Habib *J. Alloys Compd.* **209** 7 (1994)
86. N A Zakarina, G D Zakumbaeva, N F Toktabaeva *Elektrokhimiya* **19** 938 (1983)
87. R P Petukhova, G Garson Valensiya, B I Podlovchenko *Vestn. Mosk. Univ., Ser. 2, Khim.* **28** 62 (1987)
88. N Tateishi, K Yahikozawa, K Nishimura, M Suzuki, Y Iwanaga, M Watanabe, E Enami, Y Matsuda, Y Takasu *Electrochim. Acta* **36** 1235 (1991)
89. M Baldauf, D M Kolb *Electrochim. Acta* **38** 2145 (1993)
90. I Matsumura, L Sogiura, H Uchida *Z. Phys. Chem. N.F.* **164** 1545 (1989)
91. M Matsuoka, T Kohno, C Iwakura *Electrochim. Acta* **38** 787 (1993)
92. T Sakai, H Ishikawa, K Oguro, C Iwakura, H Yoneyama *J. Electrochem. Soc.* **134** 558 (1987)
93. C-N Park, M-H Chang, in *The International Symposium on Metal–Hydrogen Systems (Abstracts of Reports)* (Fujiyoshida, Japan, 1994) Mo.B6
94. M Geng *J. Alloys Compd.* **217** 90 (1995)
95. K Petrov, A A Rostami, A Visintin, S Srinivasan *J. Electrochem. Soc.* **141** 1747 (1994)
96. D-M Lee, J-Y Lu, in *The International Symposium on Metal–Hydrogen Systems (Abstracts of Reports)* (Fujiyoshida, Japan, 1994) Mo.P25
97. M Fetcenco, S Venkatesan, S Ovshinsky, in *Proceedings of the 34th International Power Sources Symposium* (New York: Cherry Hill, 1990) p. 305
98. H H Van Mal, K H J Buschow, A R Miedema *J. Less-Common Met.* **35** 65 (1974)
99. T Kitamura, C Iwakura, H Tamura *Electrochim. Acta* **27** 1723 (1982)
100. I V Kovrigina, E I Shkol'nikov, S Ya Vasina, Yu M Vol'fkovich *Vestn. Mosk. Univ., Ser. 2, Khim.* **26** 473 (1985)
101. I V Kovrigina, I L Gogichadze, S Ya Vasina, O A Petrii, E I Shkol'nikov, Yu M Vol'fkovich, in *Problemy Termodinamiki, Kinetiki i Massoperenosa v Elektrokhimicheskoi Energetike* (The Problems of Thermodynamics, Kinetics, and Mass Transfer in Electrochemical Energetics) (Moscow: Izd. Mosk. Energetich. Inst., 1986) No. 95, p. 84
102. M Matsuoka, M Terashima, C Iwakura *Electrochim. Acta* **38** 1087 (1993)
103. A Züttel, F Meli, L Schlapbach *J. Alloys Compd.* **209** 99 (1994)
104. H Sawa, M Ohta, H Nakano, S Wakao *Z. Phys. Chem. N.F.* **164** 1527 (1989)
105. S-R Kim, J-Y Lu *J. Alloys Compd.* **185** L.1 (1992)
106. T Kitamura, C Iwakura, H Tamura *Chem. Lett.* 965 (1981)
107. Kh B Shao, S Ya Vasina, I I Korobov, O A Petrii *Elektrokhimiya* **32** (1996) (in the press)

108. O A Petrii, S Ya Vasina, I L Gogichadze, in *The Xth International Congress of Metallic Corrosion (Ext. Abstracts)* (Madras, India, 1987) p. 335
109. H Sawa, M Ohta, M Hiroaki, S Wakao *Z. Phys. Chem. N. F.* **164** 1527 (1989)
110. S Fukushima, H Tanabe *Int. J. Hydrog. Energy* **8** 33 (1983)
111. O A Petrii, I L Gogichadze, S Ya Vasina, in *Dvoinoi Sloi i Adsorbtsiya na Tverdykh Elektrodakh (Tez. Dokl.)* [Double Layer and Adsorption on Solid Electrodes) (Abstracts of Reports)] (Tartu: Izd. Tartusk. Univ., 1985) Vol. 7, p. 263
112. M H Miles *J. Electroanal. Chem. Interfacial Electrochem.* **60** 89 (1975)
113. T Maoka, M Enyo *Electrochim. Acta* **26** 607 615 (1981)
114. P Los, A Lasia, *J. Electroanal. Chem. Interfacial Electrochem.* **333** 115 (1992)
115. M Enyo *Electrochim. Acta* **39** 1715 (1994)
116. K Machida, M Enyo, G Adachi, J Shiokawa *Electrochim. Acta* **29** 807 (1984)
117. K Machida, M Enyo, I Toyoshima, K Miyahara, K Kai, K Suzuki *Bull. Chem. Soc. Jpn.* **56** 3393 (1983)
118. C Iwakura, M Matsuoka, T Kohno *J. Electrochem. Soc.* **141** 2306 (1994)
119. R V Bucur, V Mecea, T Flanagan *Surf. Sci.* **54** 77 (1976)
120. A I Fedorova, A N Frumkin *Zh. Fiz. Khim.* **27** 247 (1953)
121. L Gao, B E Conway *Electrochim. Acta* **39** 1681 (1994)
122. Yu G Chirkov, V N Zhuravleva, K V Shnepelev, A G Pshenichnikov *Elektrokhimiya* **24** 1305 (1988)
123. Yu G Chirkov, A G Pshenichnikov *Elektrokhimiya* **26** 864 (1990)
124. Z-P Li, Y-Q Lei, C-P Chen, J Wu, Q-D Wang *J. Less-Common Met.* **172 – 174** 1260 (1991)
125. Q M Yang, M Ciureanu, D H Ryan, J O Strom-Olsen *J. Electrochem. Soc.* **141** 2108 2113 (1994)
126. Yu M Vol'fkovich, O A Petrii, A A Zaitsev, I V Kovrigina *Vestn. Mosk. Univ., Ser. 2, Khim.* **29** 173 (1988)
127. M Viitanen *J. Electrochem. Soc.* **140** 936 (1993)
128. R V Bucur, I Covaci *Electrochim. Acta* **24** 1213 (1979)
129. R V Bucur, F Bota *Electrochim. Acta* **27** 521 (1982)
130. Yu M Vol'fkovich, T K Zolotova, S L Bobe, A V Shlepakov *Elektrokhimiya* **29** 897 (1992)
131. R Kirchheim, F Sommer, G Schluckebier *Acta Metall.* **30** 105 (1982)
132. J O Strom-Olsen, Y Zhao, D H Ryan *J. Less-Common Met.* **172 – 174** 982 (1991)
133. J H Weaver, A Franciosi, W E Wallace, S H Kevin *J. Appl. Phys.* **51** 5847 (1980)
134. K Machida, M Enyo *J. Res. Inst. Catal. Hokkaido Univ.* **32** 737 (1984)
135. D-Y Yan, G Sandrock, S Suda, in *The 46th Annual Meeting of the International Society of Electrochemistry (Extended Abstracts)* (Xiamen, China: Xiamen University Press, 1995) Abstr. 6 – 52
136. Yu A Chizmadzhev, V S Markin, M R Tarasevich, Yu G Chirkov *Makrokinetika Protsessov v Poristykh Sredakh* (Macrokinetics of Processes in Porous Media) (Moscow: Nauka, 1971)
137. Yu M Vol'fkovich, E I Shkol'nikov *Elektrokhimiya* **19** 656; 757; 1199; 1312 (1983)
138. I G Gurevich, Yu M Vol'fkovich, V S Bagotskii *Zhidkostnye Poristye Elektrody* (Liquid Porous Electrodes) (Minsk: Nauka i Tekhnika, 1974)
139. C Iwakura, I Kim, N Matsui, H Inoue, M Matsuoka *Electrochim. Acta* **40** 561 (1995)
140. S Ya Vasina, S A Stuken, O A Petrii, I L Gogichadze, V A Mukhin *Elektrokhimiya* **23** 1127 (1987)
141. D E Hall, J M Sarver, D O Goothard *Int. J. Hydrog. Energy* **13** 547 (1988)
142. V S Bagotskii, N V Osetrova *Elektrokhimiya* **31** 453 (1995)
143. D T Hughes, I R Harris *J. Less-Common Met.* **61** 9 (1978)
144. M L Doyle, I R Harris *Platinum Metals Rev.* **32** 130 (1988)
145. C J Lihn, C C Wan, T P Perng *J. Appl. Electrochem.* **25** 61 (1995)
146. G A Tsirlina, M Yu Rusanova-Berdonosova, V A Roznyatovskii, O A Petrii *Elektrokhimiya* **31** 25 (1995)
147. M Nogami, M Tadokoro, M Kimoto, Y Chikano, I Ise, N Furukawa *Denki Kagaku* **61** 1088 (1993)
148. S Srinivasan, W Zhang, M P Kumar, A Visintin, in *The 46th Annual Meeting of the International Society of Electrochemistry (Extended Abstracts)* (Xiamen, China: Xiamen University Press, 1995) Abstr. 5 – 44
149. J Chen, in *The 46th Annual Meeting of the International Society of Electrochemistry (Extended Abstracts)* (Xiamen, China: Xiamen University Press, 1995) Abstr. 5 – 38